

## 2.3. PHYSICAL COVARIATE DATA

### 2.3.1. Data Processing

After accounting for redundancy among the collated data, and collapsing the monthly SeaWiFS data to annual average and variability, there were 21 covariates (+8 measures of variability in the CARS & SeaWiFS attributes) for developing bio-physical models of biological survey data and for stratification of the TS non-reef region. These datasets were checked and imported into an ArcInfo GIS.

We constrained the covariates to the continental shelf by establishing a base study area bounded by the Torres Strait Protected Zone and adjacent areas but excluding those areas beyond the continental shelf.

A 36-arc-second grid (0.01 decimal degree, (~1.11 km)) was generated for this area. Each grid cell was assigned a unique identifier that was subsequently used as the key to this dataset. As the collated data were of various spatial resolutions, we resampled those data to the 36-arc-second grid framework by a discrete thin plate spline technique (Wahba, 1990) using the TOPOGRID module in ArcInfo, to provide a consistent set of full-coverage covariates for the Project. As many of the covariates were not available for every grid cell, a “reliability indicator” was calculated that represented the distance to the nearest source data.

The TS wide coverage of all of the collated covariates was thematically mapped using a colour range appropriate to the individual distribution.

The interpolated physical data for each grid cell were exported out of ArcInfo for statistical analysis. This physical data set was also geographically matched to the location of each sampling station in the Biological Survey datasets. These were also exported from the ArcInfo GIS into a database suitable to provide physical covariates matching biological sample data for statistical analyses of bio-physical relationships.

### 2.3.2. Maps of Physical Covariate Data

#### 2.3.2.1. Bathymetry

Torres Strait is a complex shallow area of continental shelf between Cape York and Papua New Guinea (Figure 2.3-1) (Harris, 1995). The main features are two central ridge lines extending from Cape York to PNG, coming to the surface at numerous places as reefs and islands, and dissected by numerous channels. In the far east, the Great Barrier Reef extends northward onto the PNG shelf at the

western extremity of the Gulf of Papua. Outside the barrier, the slope drops very steeply into 2,000-4,000 m depths. In eastern Torres Strait, behind the barrier, there are numerous shallow reefs and in the northeast, these form large complexes dissected by deep channels. These deep channels, and those just south of the PNG coastline, are old river beds that continue to be scoured by tidal currents. Western Torres Strait grades gently into the Gulf of Carpentaria. Northwest Torres Strait is very shallow and mostly un-navigable by hydrographic vessels.

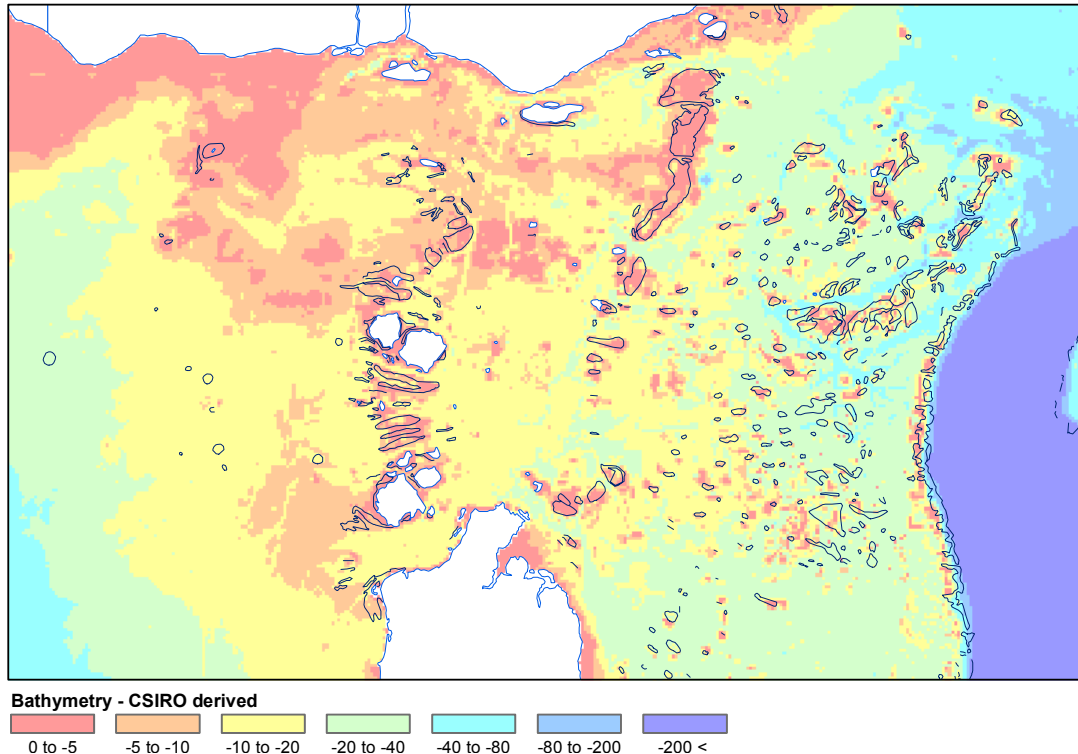


**Figure 2.3-1** DEM of the bathymetry (m) of Torres Strait, mapped onto a 0.01° grid, from various sources (see section 2.1.1).

The bathymetry of the major shipping channels of Torres Strait is well surveyed for navigation purposes (Figure 2.3-2, dark blue areas through Prince of Wales, Adolphus and Great NE Channels). Much of the remainder of Torres Strait, however, is poorly mapped and potentially unreliable for bio-physical mapping. Areas of particular concern in this regard include: NE Torres Strait, which is very complex with large formations of reefs and shoals, deep areas and even deeper channels; and NW Torres Strait, which is very shallow with complex sand ridges and shoals mostly uncharted.

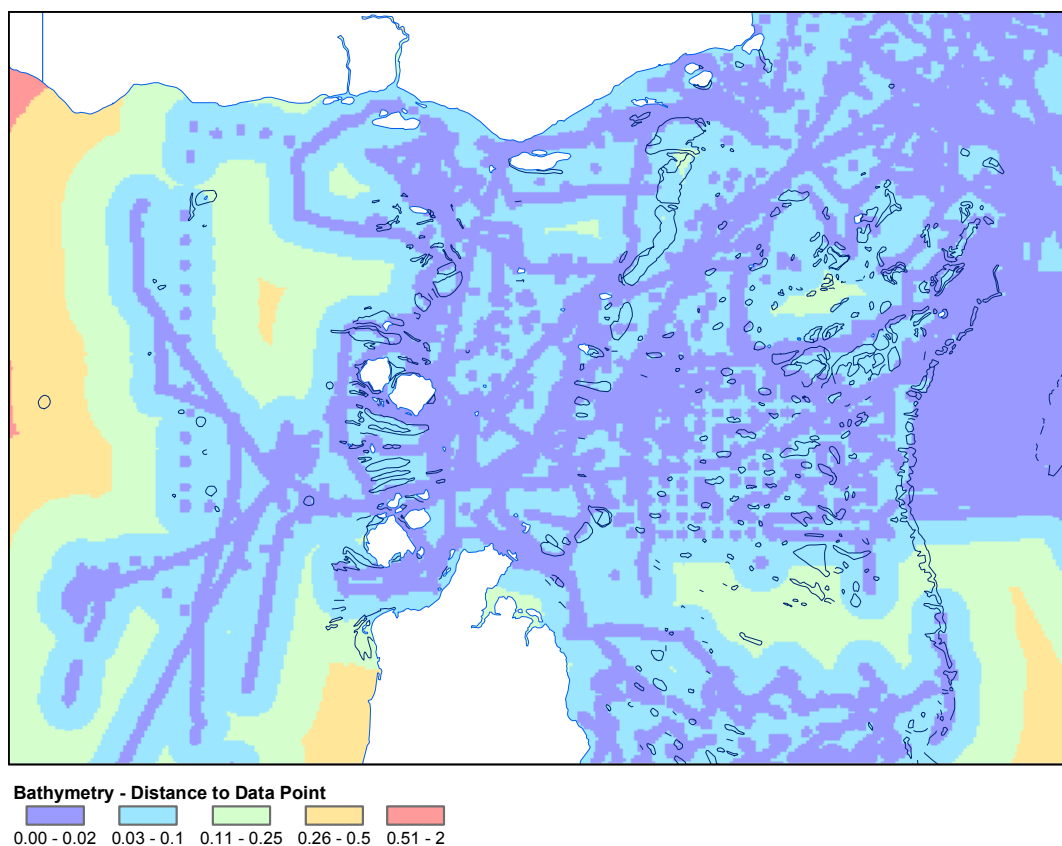


**Figure 2.3-2** Map of distance (decimal degrees) to soundings, mapped onto a 0.01° grid, as an indication of bathymetric reliability and data gaps for Torres Strait.

#### 2.3.2.2. *Sediment Attributes*

The surface sediments of Torres Strait are a reflection of the terrestrial inputs, particularly from major river systems such as the Fly in the NE, and biogenic production of carbonate skeletons by foraminiferans, bryozoans, algae and corals, modified by strong tidal currents, particularly in narrow channels between reefs, and sea level change during periods of glaciation (Harris, 1991, 1995). High mud areas include: off the Fly River delta, west of Warrior Reef, the Great NE Channel, and east of Cape York (Figure 2.3-3). Gravel especially dominates areas between reefs and islands where strong tidal currents scour finer sediments away, depositing them in dunes beyond the channels, leaving gravel and/or pavement (Figure 2.3-3) (Harris, 1991). Rock is distributed similarly to gravel, but is more constrained (Figure 2.3-3). The sand fraction is most ubiquitous, dominating wherever mud, gravel and rock do not (Figure 2.3-3). Characteristic grain size reflects the distribution of the sediment fractions coarse (red) to fine (blue), and grain sorting indicates the range of grain size from homogeneous (blue) to widely mixed sizes (red) (Figure 2.3-3). The composition of most of Torres Strait sediments is carbonate, with low carbonate areas close to Cape York and PNG indicating the input of terrestrial sediments (Figure 2.3-5).

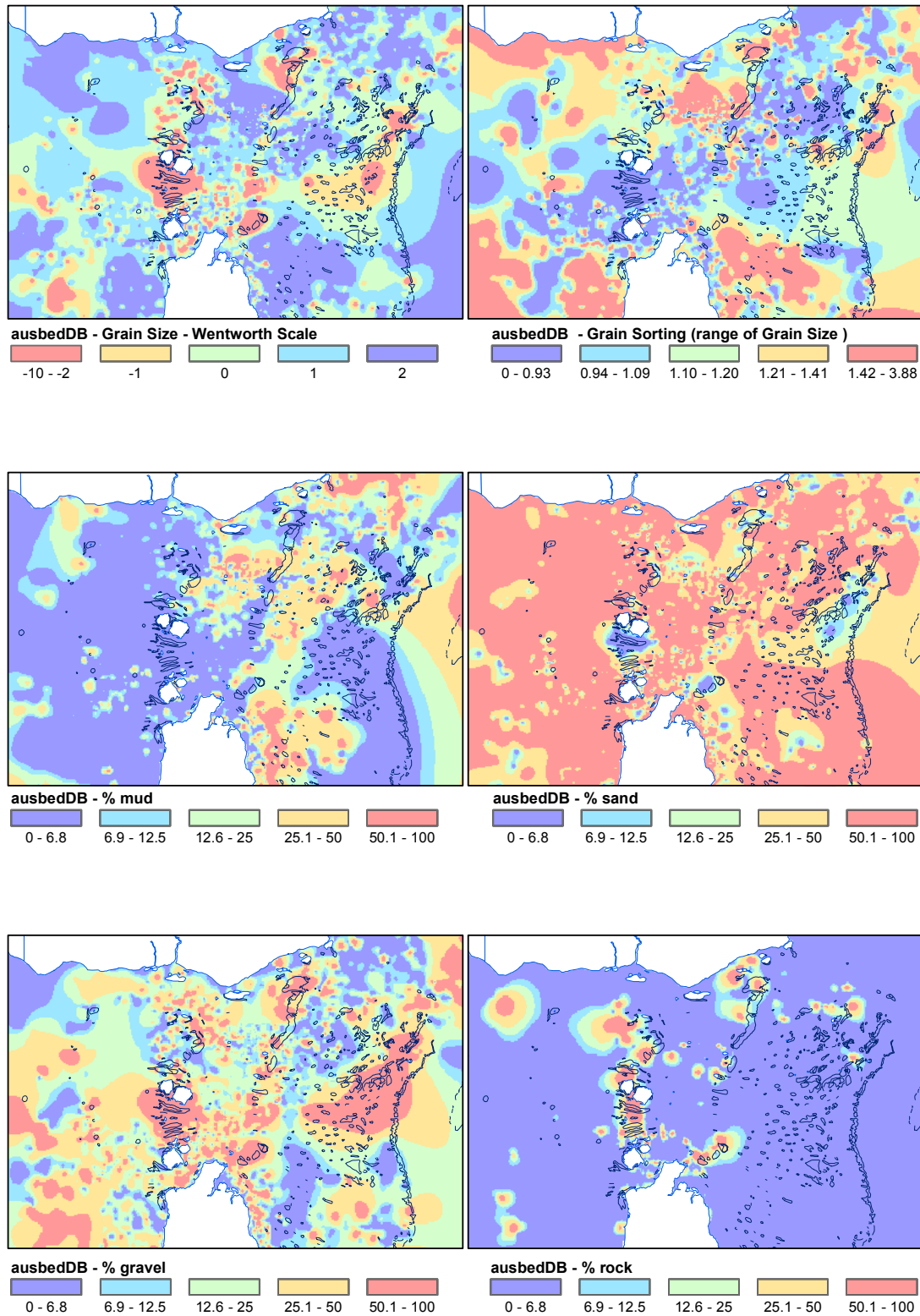


**Figure 2.3-3** Maps of sediment grain size attributes for Torres Strait: characteristic grain size, sorting, and percent mud/sand/gravel/rock fractions (source, see section 2.1.1).

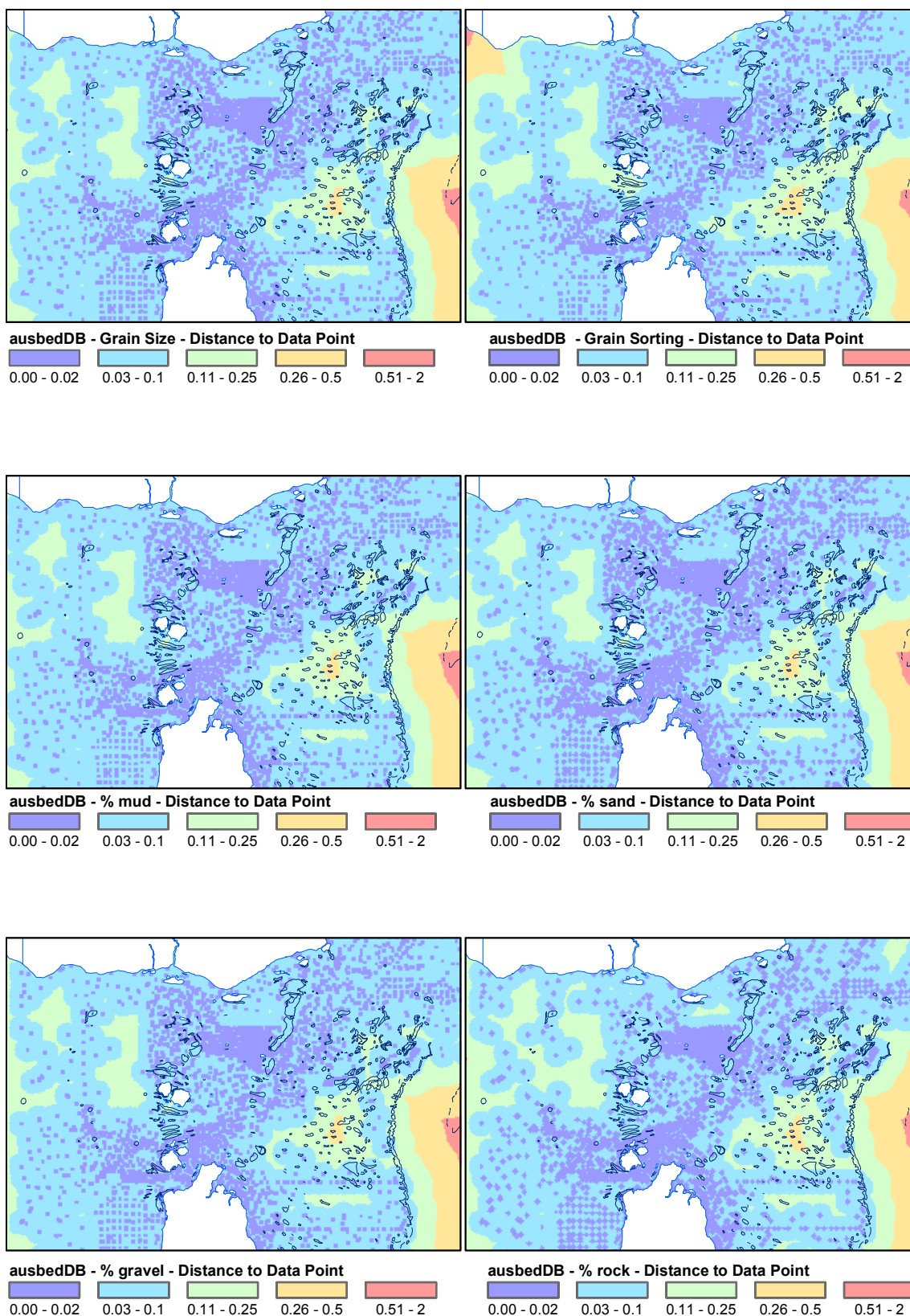


**Figure 2.3-4** Map of distance (decimal degrees) to sample sites for sediment attributes, mapped onto a 0.01° grid, as an indication of reliability and data gaps for sediment attributes in Torres Strait.



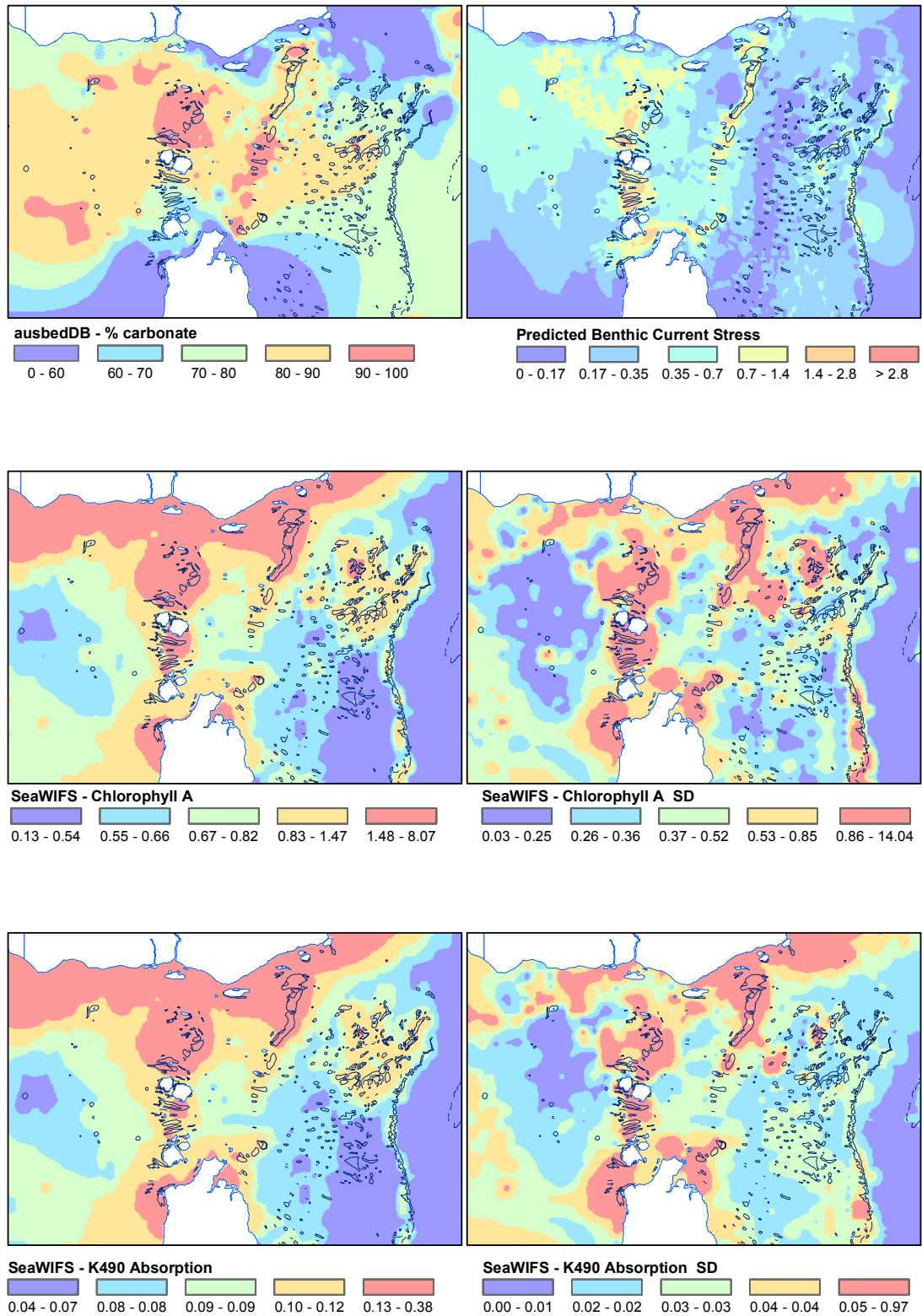
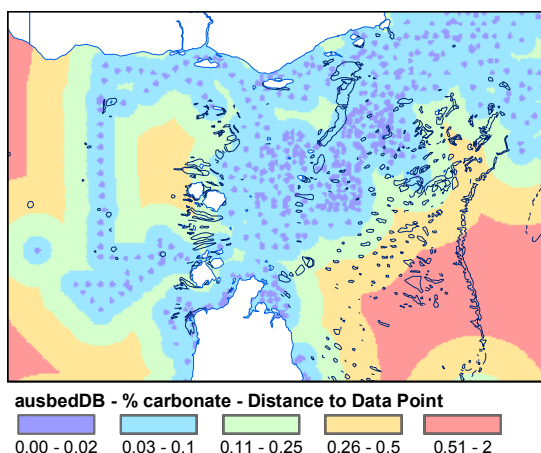


**Figure 2.3-5** Maps of sediment carbonate composition, mean modeled seabed current stress, SeaWiFS predicted chlorophyll-a and standard deviation, and light absorption (attenuation coefficient) at 490 nm and standard deviation for Torres Strait (sources, see section 2.1.1).



The sediment grain size attributes of the main shipping channels and of an area west of the southern warrior reefs have been relatively well sampled (Figure 2.3-4), whereas as most of eastern and northwestern Torres Strait are largely unsampled. The remainder has been only patchily and inadequately sampled. The gaps for carbonate data are even more significant (Figure 2.3-6).

**Figure 2.3-6** Map of distance (decimal degrees) to sample sites for sediment carbonate, mapped onto a 0.01° grid, as an indication of reliability and data gaps for this sediment attribute in Torres Strait.

### 2.3.2.3. Seabed Current Stress

The physical oceanography of Torres Strait is dominated by the tidal regime, which generates extremely strong currents. These tidal currents are driven by the Coral Sea/Gulf of Papua and Gulf of Carpentaria/Arafura Sea tidal cycles, which are largely out of phase causing large sea level gradients across Torres Strait (Bode & Mason, 1995; section 2.2.1). The tidal currents exert a force on the seabed, that in turn causes friction to the flow of water, known as seabed current shear stress, which redistributes sediments (Harris, 1991, 1995) and appears to influence biotic assemblages (section 2.7).

The areas of highest seabed stress occur where the tidal currents are forced through the narrow channels between the reefs and islands of western Torres Strait, the Warrior Reefs system, and to a lesser extent in eastern Torres Strait and the outer barrier (Figure 2.3-5). The shallows of northwestern Torres Strait are an extensive area of moderately high current stress (Figure 2.3-5) that transports sediments and forms large dunes and sand banks (Harris, 1991, 1995). The higher stress areas correspond with larger grain size fractions and, conversely, low stress areas correspond with finer grain size fractions (cf. Figure 2.3-3). The higher stress areas also correspond with the occurrence of benthic sponge and gorgonian gardens (Figure 2.4-2, Figure 2.4-3, Figure 2.4-4).

The reliability of the seabed current stress data is dependent on the availability of bathymetric data, which has significant gaps (section 2.3.2.1), and on the resolution and accuracy of the current modelling (Bode & Mason, 1995). There are few tidal and current monitoring stations in Torres Strait (section 2.2) against which to test model results, nevertheless, those that do exist correspond well (Bode & Mason, 1995).

### 2.3.2.4. Ocean Colour (chlorophyll & turbidity)

The use of SeaWiFS ocean colour data for estimating chlorophyll is discussed in section 2.2.4, and seasonal patterns are presented there. The annual mean and standard deviation (indicating seasonal variability) of estimated chlorophyll and turbidity (attenuation coefficient at 490 nm) are shown in Figure 2.3-5. The strong correlation between these remote sensed estimates can be readily seen, and is an issue for the reliability of this data (section 2.2.4).

#### 2.3.2.5. *Bottom Water Attributes*

The CARS database of hydrographic measurements was discussed in detail in section 2.2.2, including seasonal and wider regional patterns at the sea surface. This section presents the CARS mappings at the seabed for the Torres Strait study area, as used in section 2.7. Unfortunately, there is very little oceanographic data for Torres Strait (Furnas, 1991; section 2.2.2), so the mappings presented here need to be considered with caution, as any apparent fine scale detail is likely to be an artefact of the interpolation.

The annual average salinity appears to be higher in western, southern and central Torres Strait, with an area of lower salinity in northern Torres Strait (Figure 2.3-7) due to riverine input from PNG, some of which originates from the Fly River (Furnas, 1991; Wolanski, 1991; section 2.2.2). The standard deviation (implied seasonal variability) appears to be higher in the northern area (Figure 2.3-7), due to the monsoonal seasonality of the riverine input. Temperature appears to be higher in western/central Torres Strait, with higher standard deviation in the same general area (Figure 2.3-7). Dissolved oxygen appears to be higher in central/northern Torres Strait, corresponding with the shallow areas of high tidal current energy. The higher oxygen areas seem to be seasonally consistent with low standard deviation in the same general area; areas with large standard deviation occur in eastern Torres Strait (Figure 2.3-7). There is likely to be tidally driven upwelling at the shelf break in eastern Torres Strait that may inject cooler water and nutrients onto the shelf seabed behind the barrier reef (Wolanski, 1991).

The concentration of silicates is an indication of the influence of terrestrial inputs (Furnas, 1991). The annual average silicate concentration tends to be higher in the area of the Great NE Channel (Figure 2.3-9) probably due to the influence of the Fly River (Furnas, 1991; Wolanski, 1991); the standard deviation of silicate also tends to be higher in this area. Nutrient levels (phosphate, nitrate) are generally low in Torres Strait (Furnas, 1991). The limited data suggest relatively higher values appear to occur in central/western areas and deep waters off the shelf, and standard deviations appear to be larger where annual means are higher (Figure 2.3-9), but these patterns need to be treated with caution (section 2.2.2).

There are broad areas of uncertainty for all bottom water attributes in Torres Strait, as indicated by the RMS residual of the mapping and scarcity of CTD casts (Figure 2.3-8, Figure 2.3-10). This is particularly so for oxygen, silicate and nutrients, but the additional once-off data for temperature and salinity offer limited improvement because of the temporal dynamics of these attributes.

#### 2.3.2.6. *Prawn Trawl Effort*

Trawling for prawns occurs in central-eastern Torres Strait, with areas of highest effort in the vicinity of Yorke Island and extending towards Coconut Island (Figure 2.3-11). This area is typified by muddy-sand and low current stress, suitable for prawns. The variability in annual effort intensity corresponds closely with the amount of effort (Figure 2.3-11).



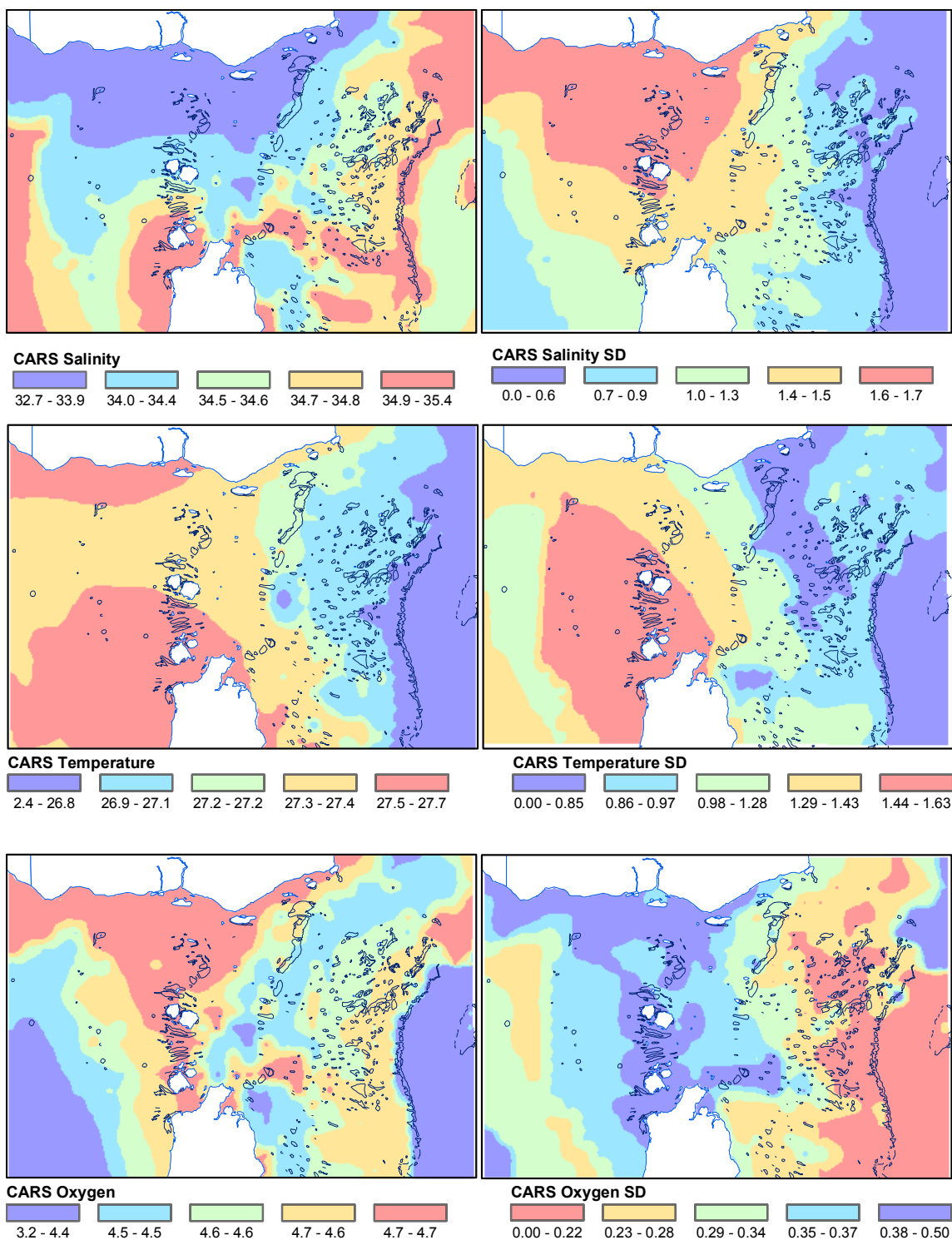


**Figure 2.3-7** Maps of CARS bottom water physical attributes for Torres Strait: salinity (mean & SD), temperature (mean & SD), and dissolved oxygen (mean & SD), (source, see section 2.1.1).

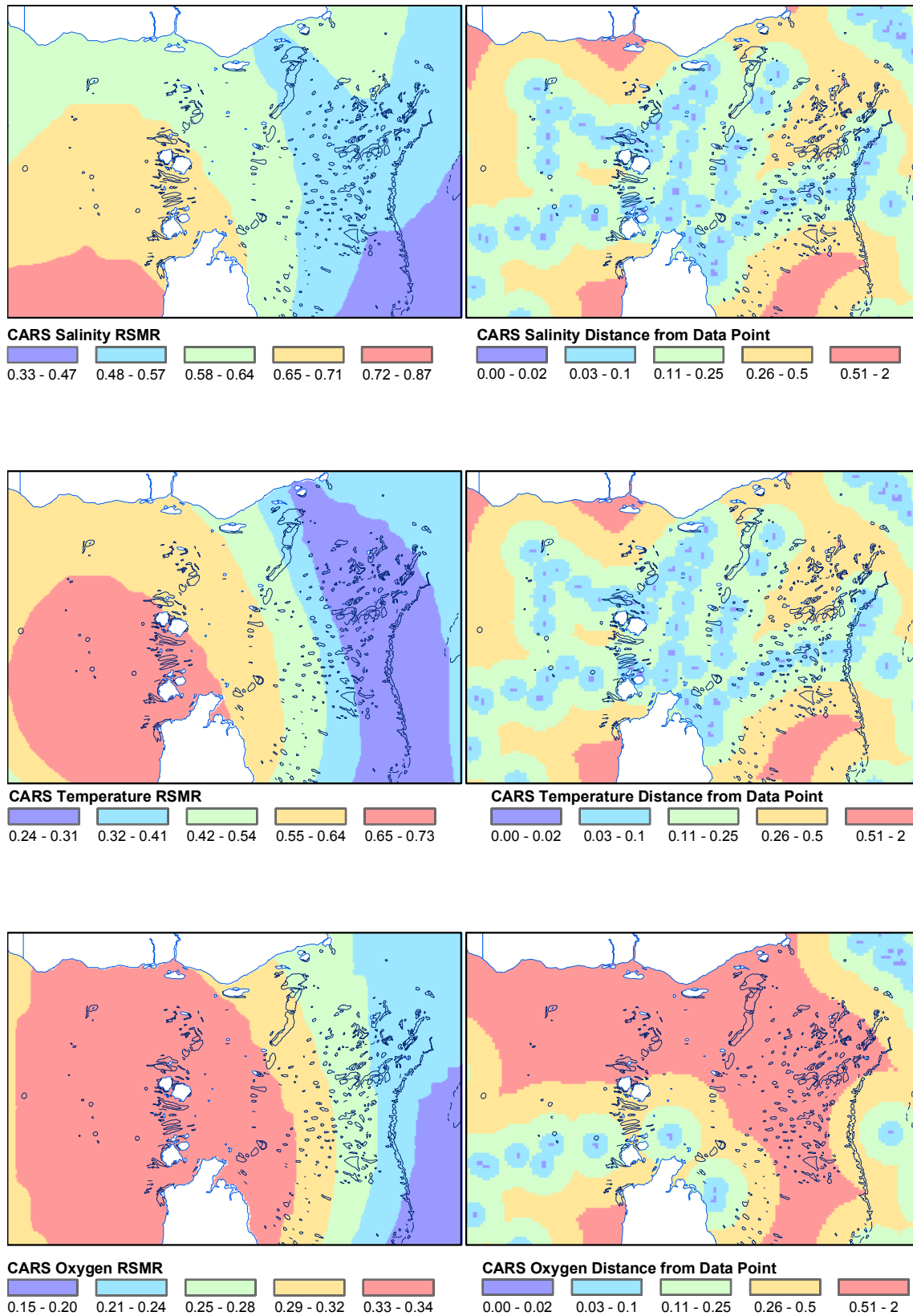


**Figure 2.3-8** Maps of root-mean-square residual of CARS mapping, and distance (decimal degrees) to CTD casts for CARS attributes, mapped onto a 0.01° grid, as an indication of reliability and data gaps for physical water attributes at the seabed in Torres Strait.

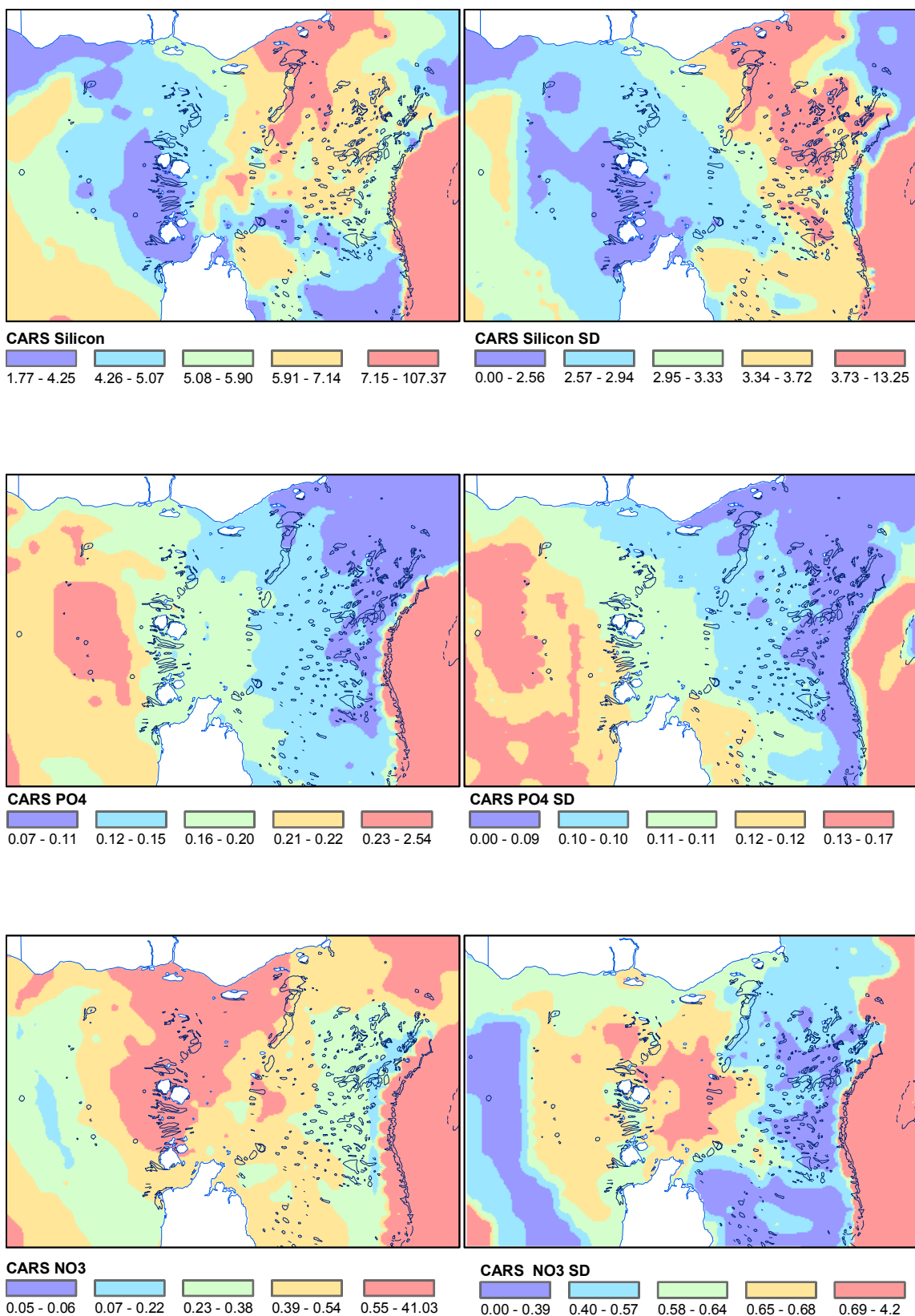


**Figure 2.3-9** Maps of CARS bottom water nutrient attributes for Torres Strait: silicate (mean & SD), phosphate (mean & SD), and nitrate (mean & SD), (source, see section 2.1.1).

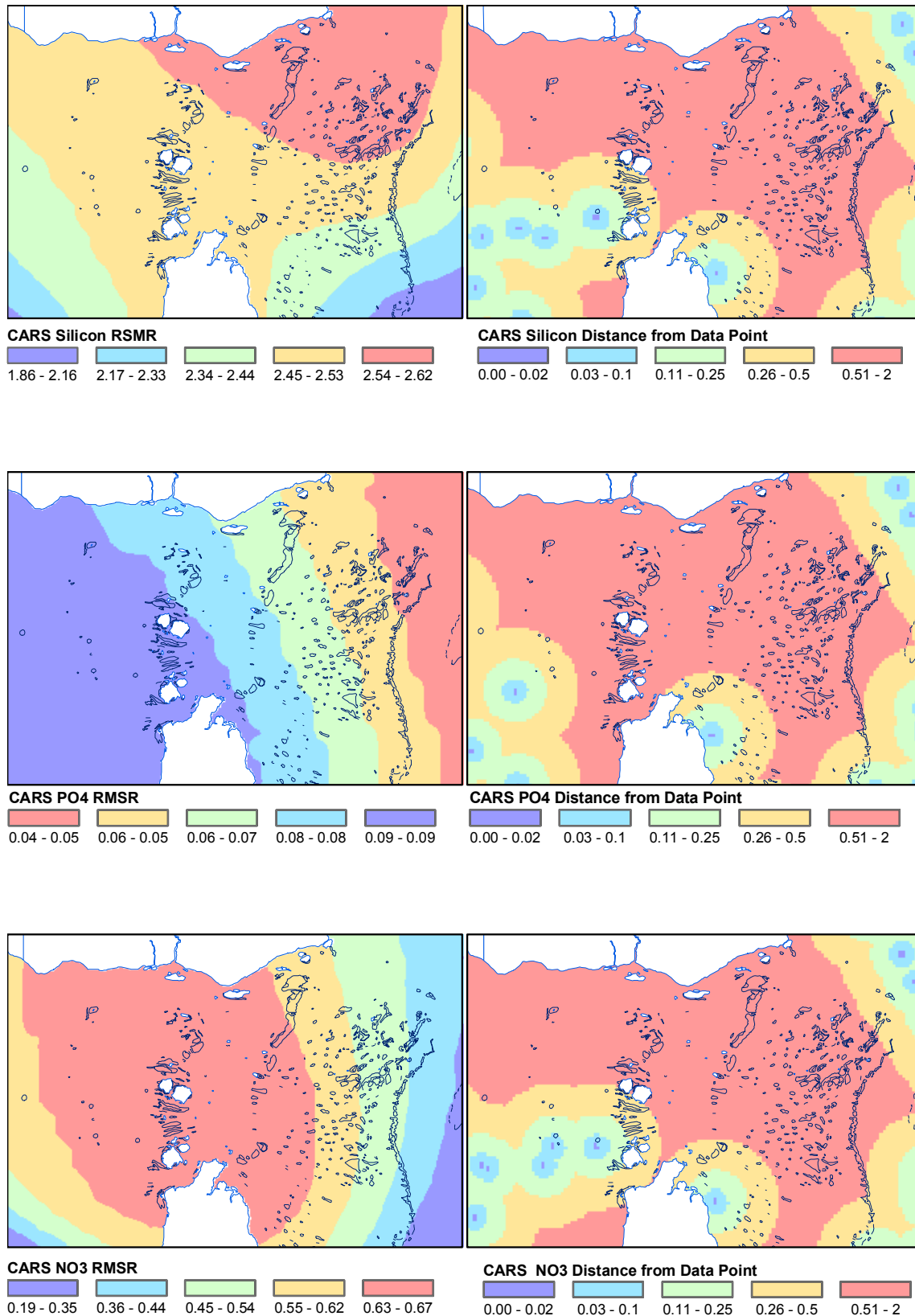


**Figure 2.3-10** Maps of root-mean-square residual of CARS mapping, and distance (decimal degrees) to CTD casts for CARS attributes, mapped onto a 0.01° grid, as an indication of reliability and data gaps for water nutrient attributes at the seabed in Torres Strait.

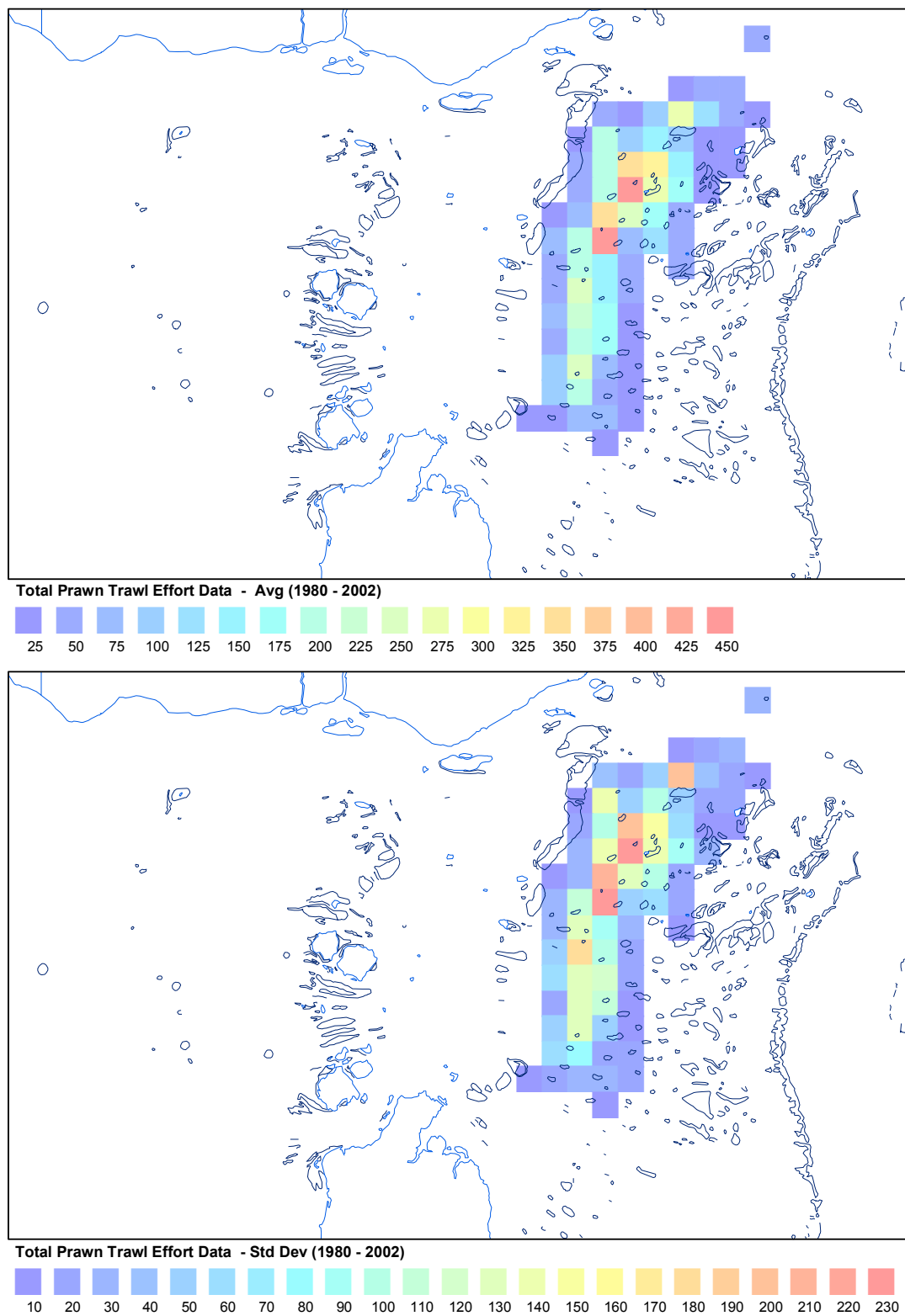


**Figure 2.3-11** Maps of Torres Strait prawn trawling effort (boat-days per 6 min grid cell), average and standard deviation for years 1980-2002 (source, see section 2.1.1).